Lectures on Conformal Bootstrap

M. F. Paulos
CERN Theory Division

D=4 bound

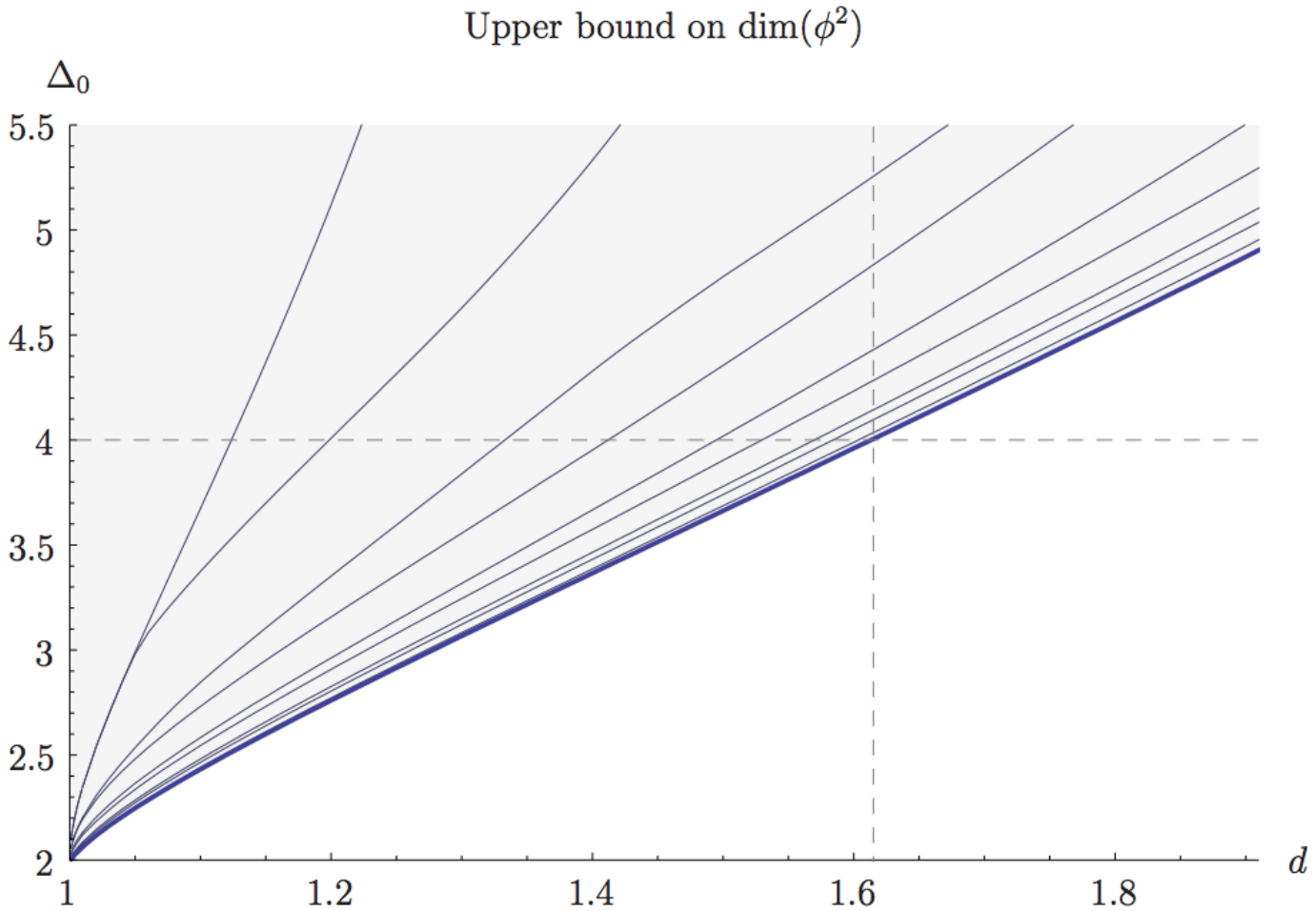

Bootstrapping $\langle\phi\phi\phi\phi\rangle$, $\Delta_\phi \equiv d$, $\Delta_0 \equiv \Delta_{\phi^2}$.

D=2 bound

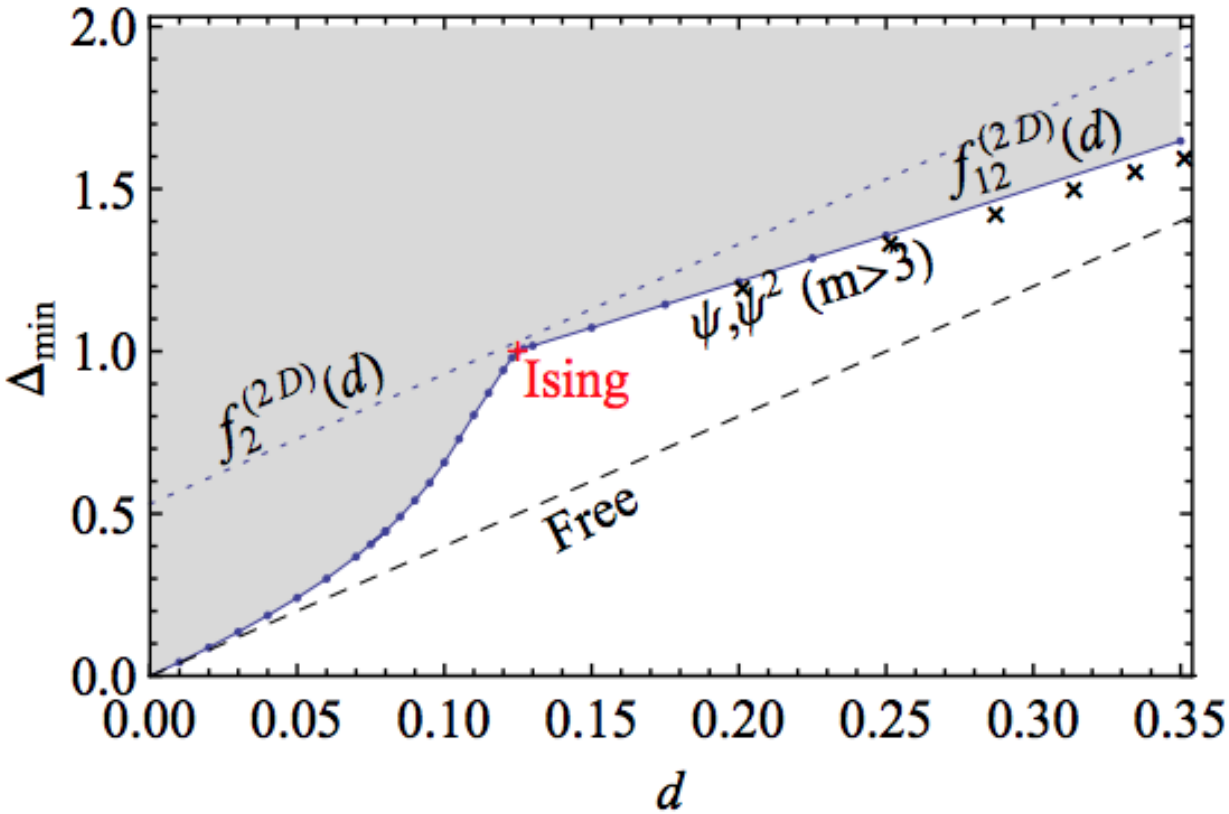

Bootstrapping $\langle\phi\phi\phi\phi\rangle$, $\Delta_\phi \equiv d$, $\Delta_{\min} \equiv \Delta_{\phi^2}$. Black crosses represent minimal model correlation functions characterized by $\simeq \mathcal{L}_{-2} + a\mathcal{L}^2_{-1} = 0$.

D=3 bound

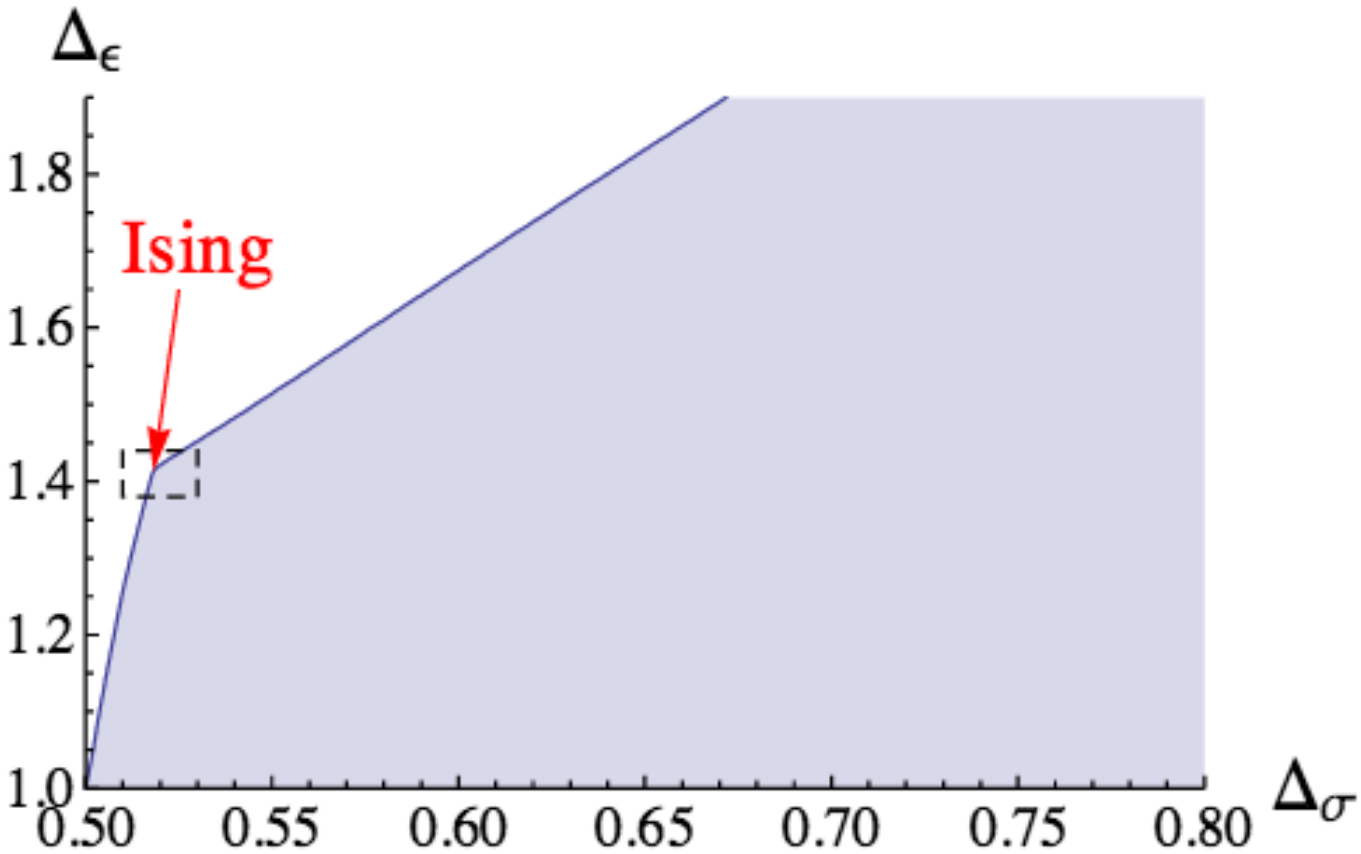

Bootstrapping $\langle\phi\phi\phi\phi\rangle$, $\Delta_\phi \equiv \Delta_\sigma$, $\Delta_\varepsilon \equiv \Delta_{\phi^2}$.

Dimension bounds in various dimensionality

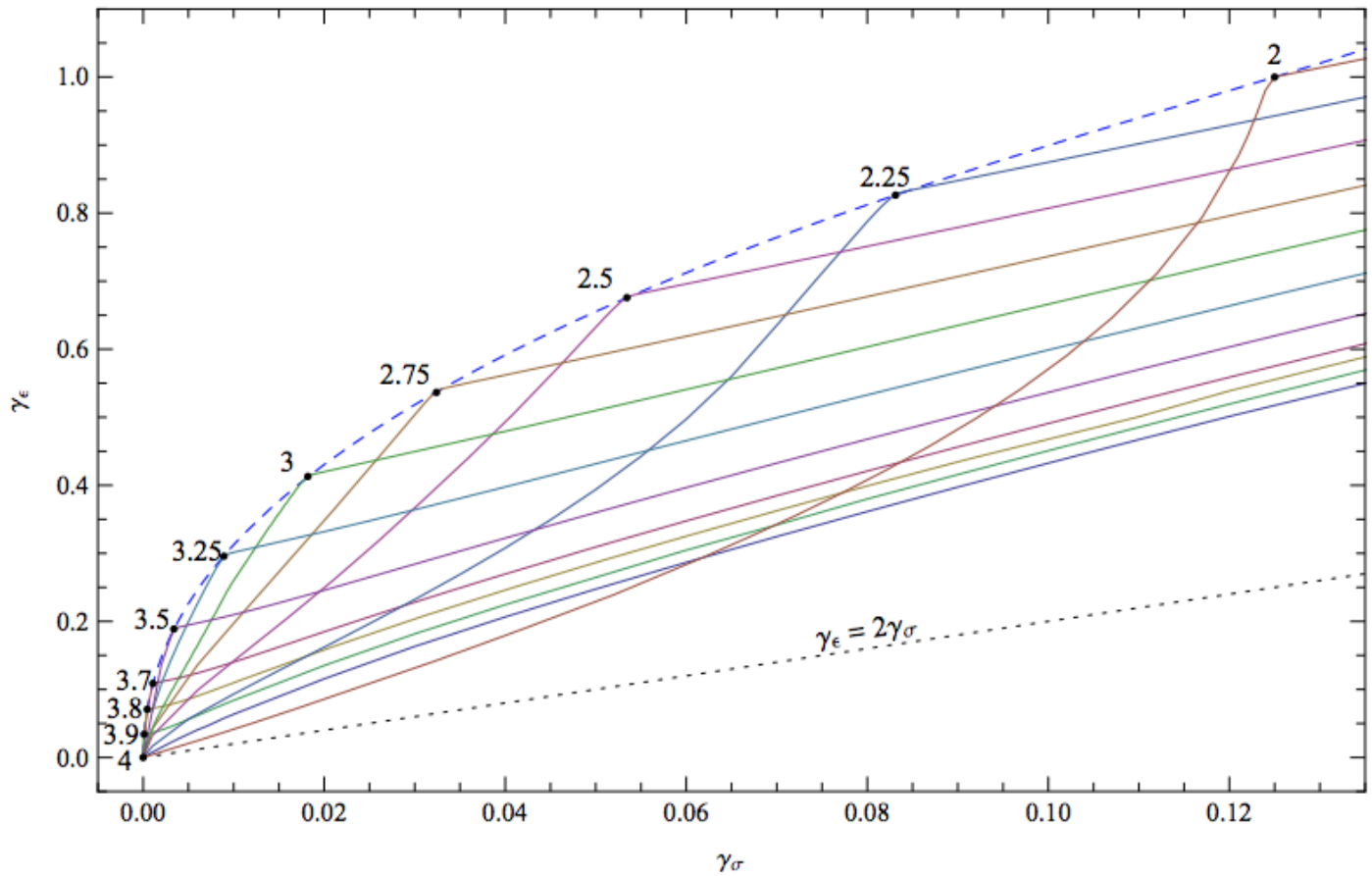

FIG. 1. Upper bounds on γ_ϵ as a function of γ_σ, plotted for $D = 2, 2.25, \ldots, 4$. For each $D < 4$, the bound shows a kink, where a CFT belonging to the Ising model universality class is conjectured to live (black dots, fitted by the blue dashed curve). An example of theories in the bulk of the allowed region are Gaussian models, where $\gamma_\epsilon = 2\gamma_\sigma$ (black dotted line).

Comparison with ϵ-expansion

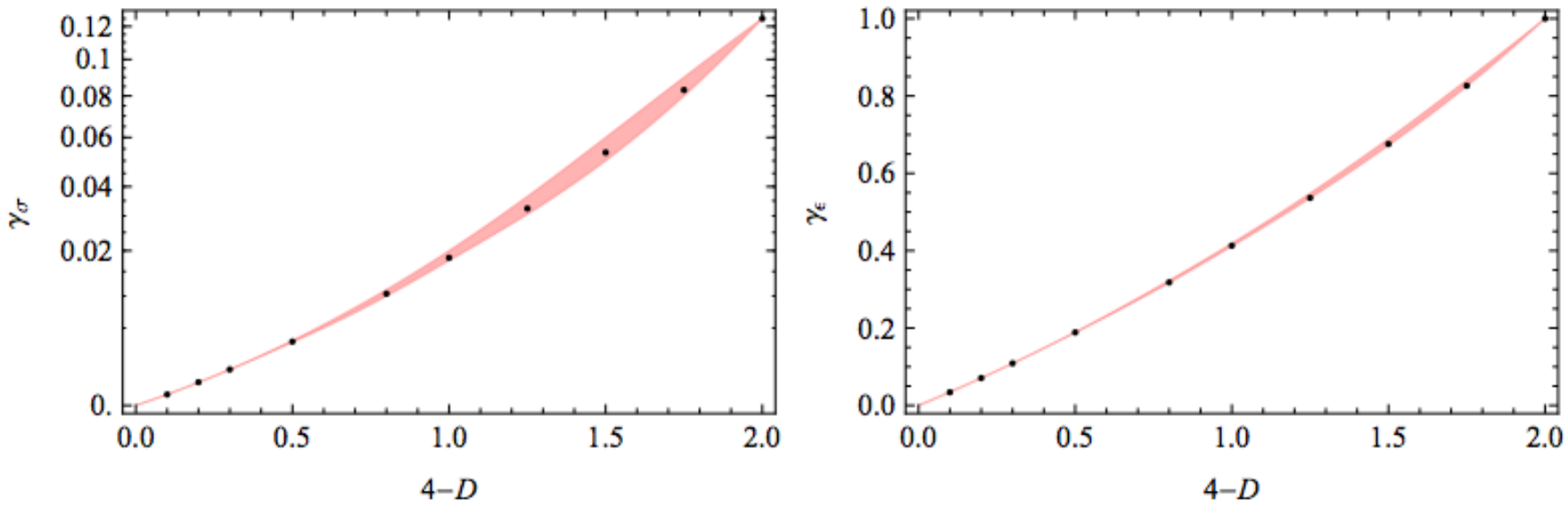

Figure: Anomalous dimensions of σ and ϵ field as a function of $4 - D$. Black dots are bootstrap results (the kinks), orange bands represent 5-loop Borel resummed ϵ-expansion.

$O(N)$ models in $D = 3$

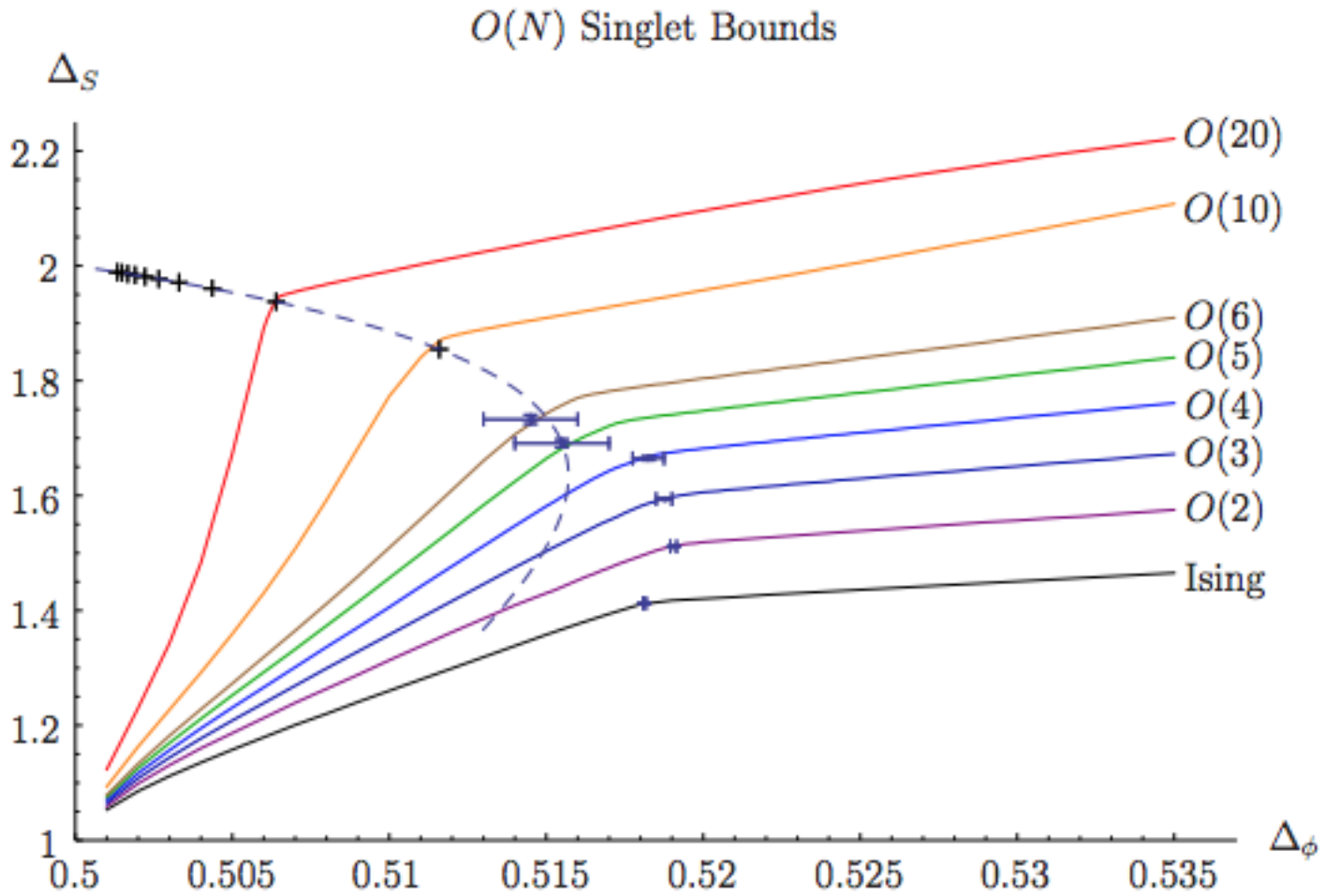

Figure: Bound on the singlet in the $\phi_i \times \phi_j$ OPE. Error bars represent best MC and analytic determinations. Black crosses are large N expansion.

Multiple correlators - 3D Ising

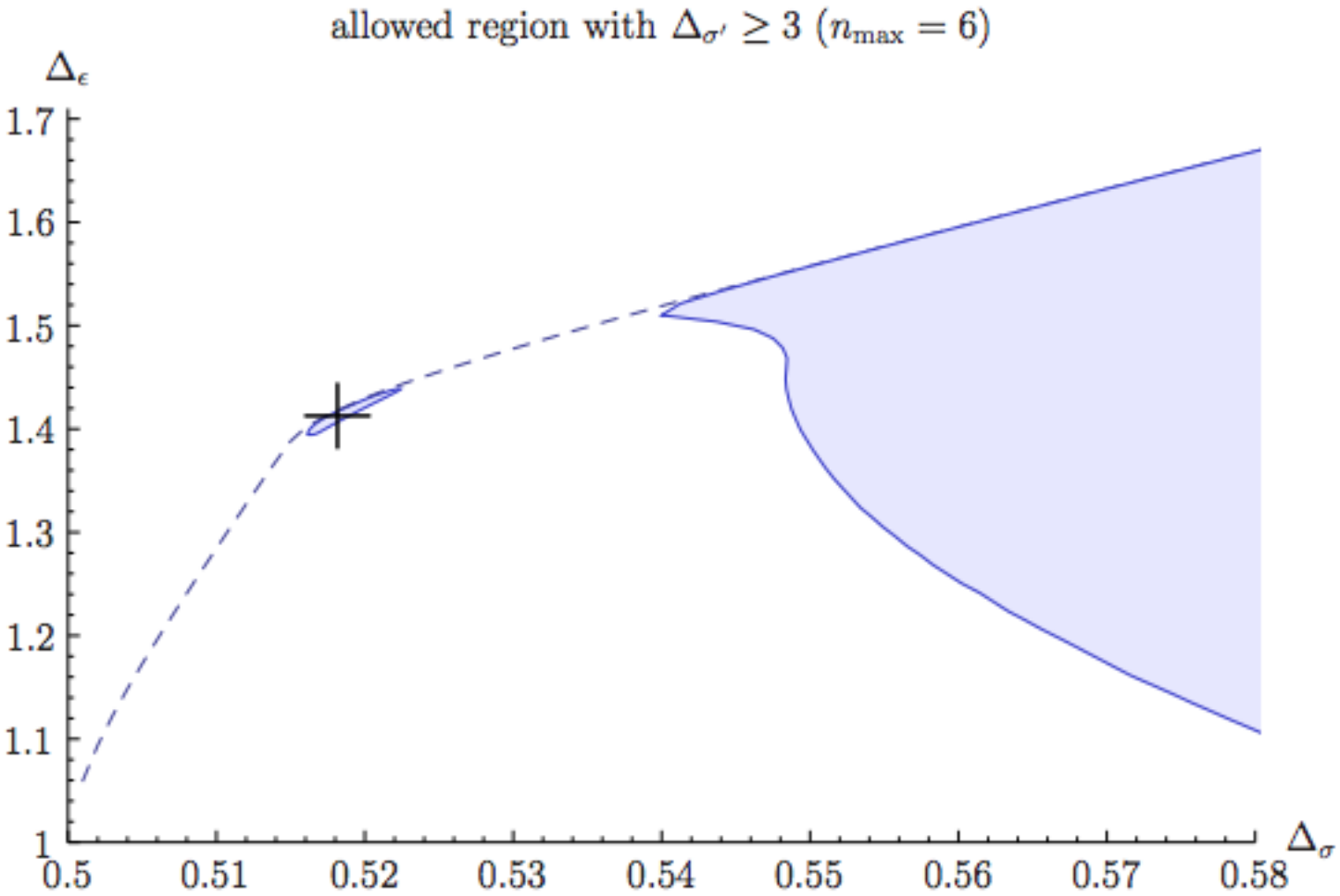

Figure: Analysis with multiple correlators (σ, ϵ fields). Includes a gap in spin-odd sector up to dimension 3 (Ising should only have one relevant even scalar).

Multiple correlators - 3D Ising

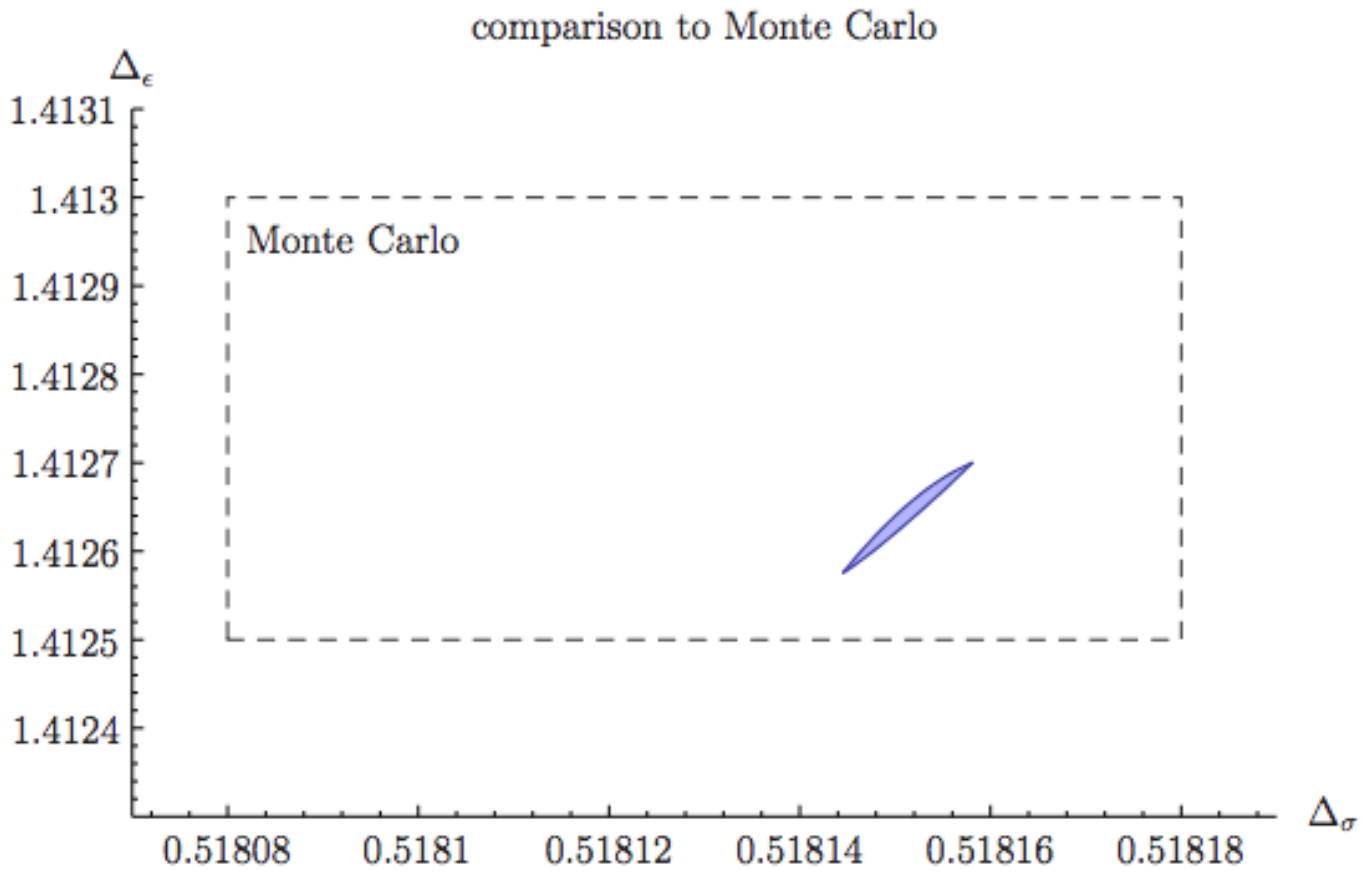

Figure: Zoom on the previous plot, more derivatives.

Multiple correlators - 3D $O(N)$

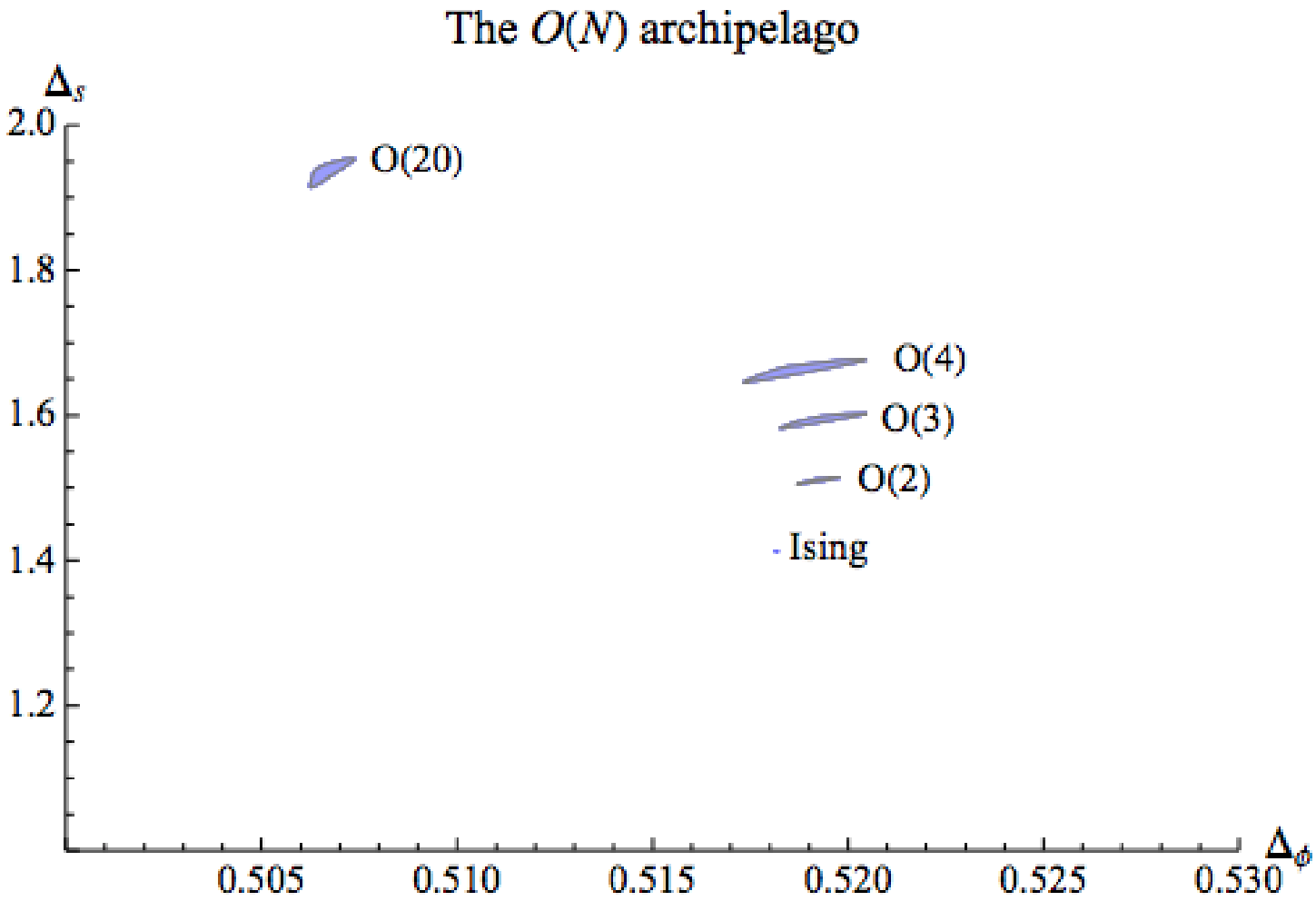

Kinks and spectra

Variation with N

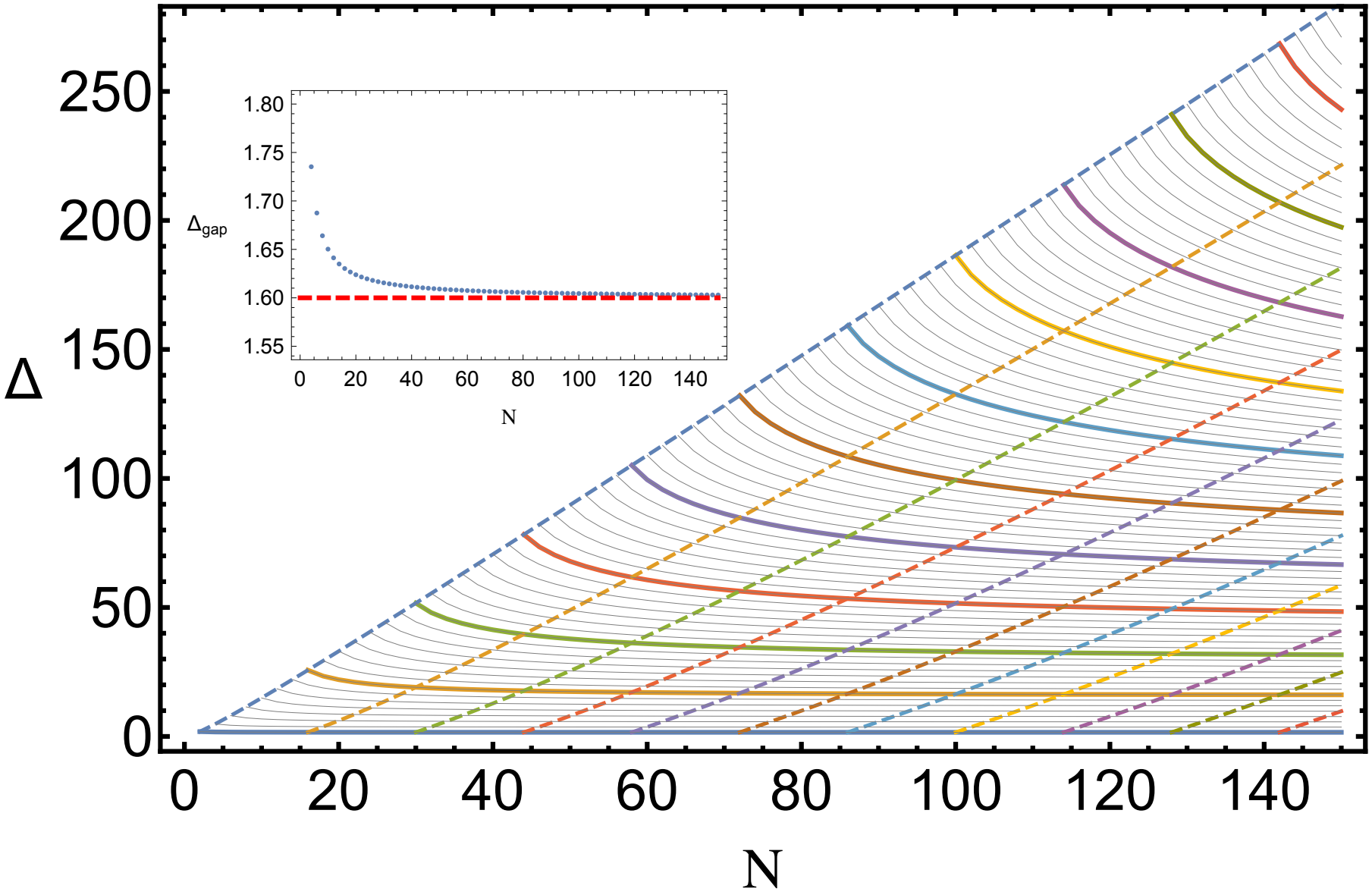

Evolution with N

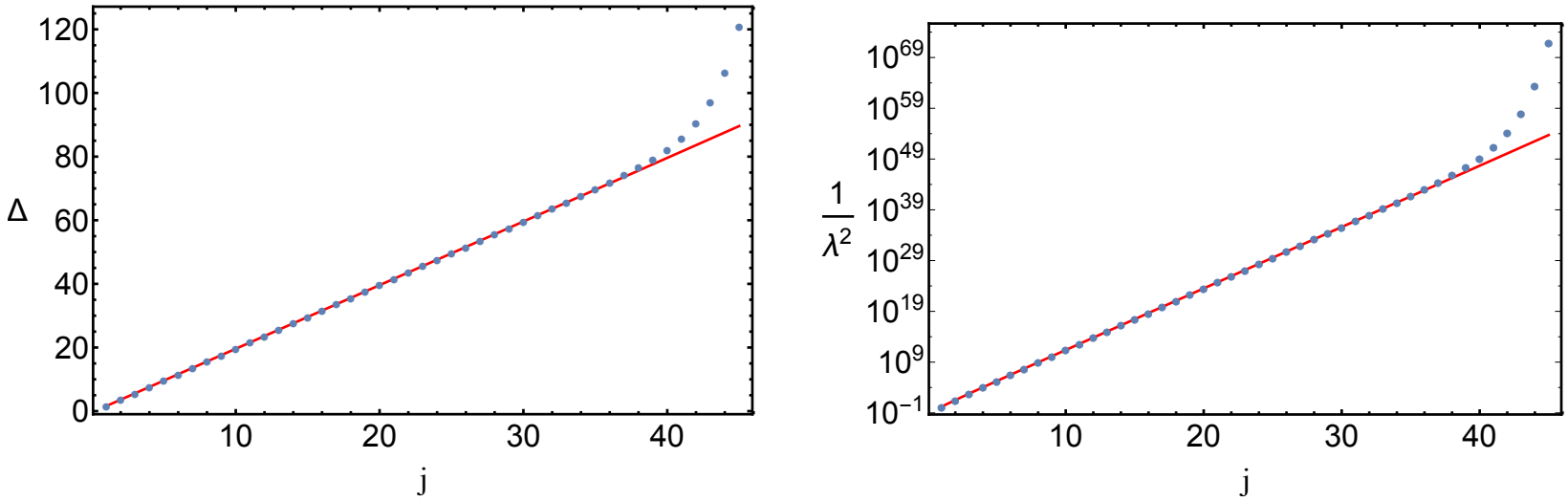

Figure: Comparison between extrapolated vs exact spectra. The exact solution is the generalized free fermion with dimensions $\Delta(j) = 1 + 2\Delta_\phi + 2j$, here evaluated at $\Delta_\phi = 0.3$. The exact values lie on the solid red line whereas the extrapolated results are represented by the blue dots.

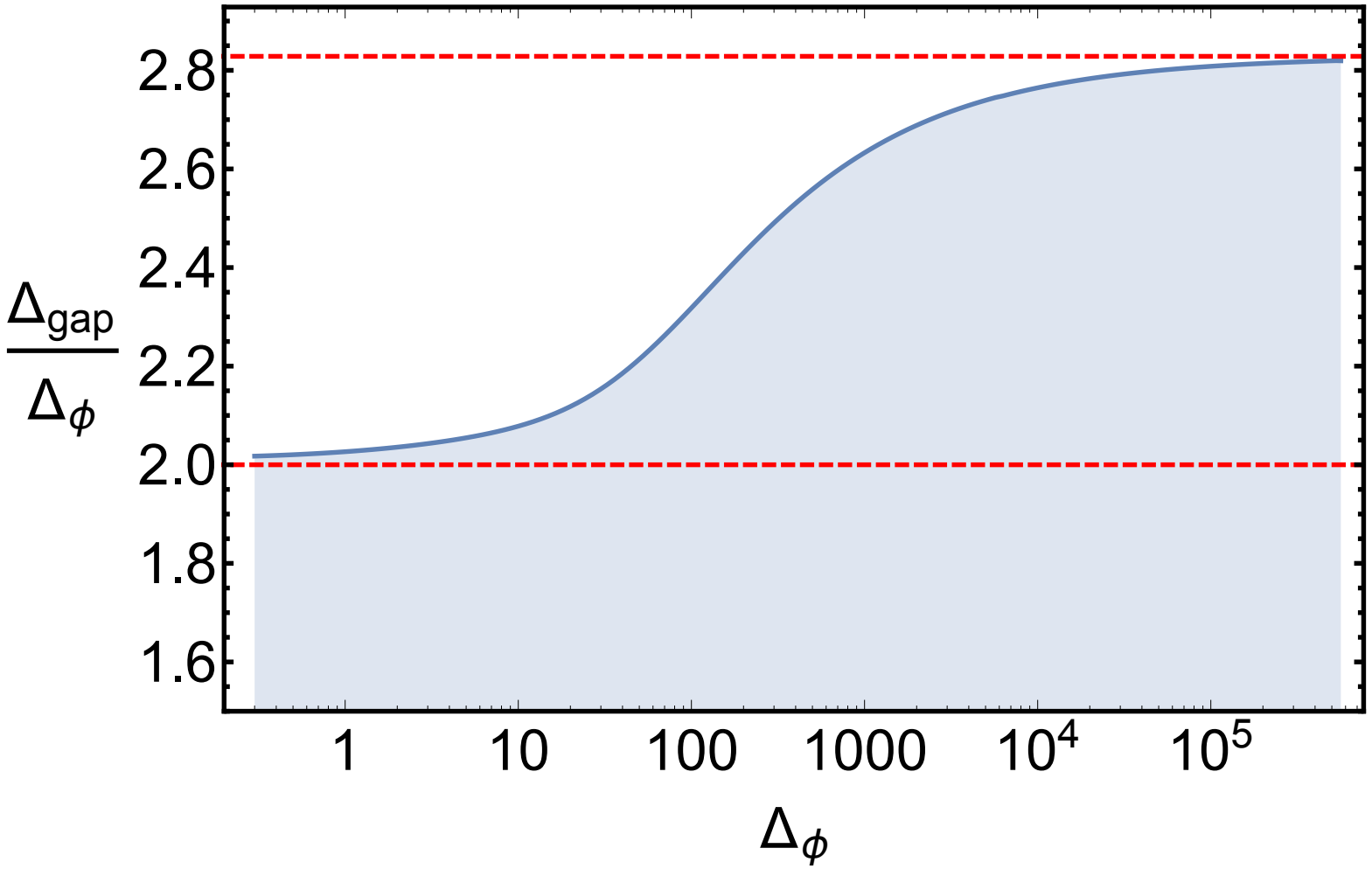

Figure: Gap maximization with 100 components. The curve provides a valid upper bound on the dimension of ϕ^2 in $D = 1$ CFTs. The slope of the bound smoothly interpolates between 2 and $2\sqrt{2}$. As the number of components increases, the transition region is pushed to higher values of Δ_ϕ.

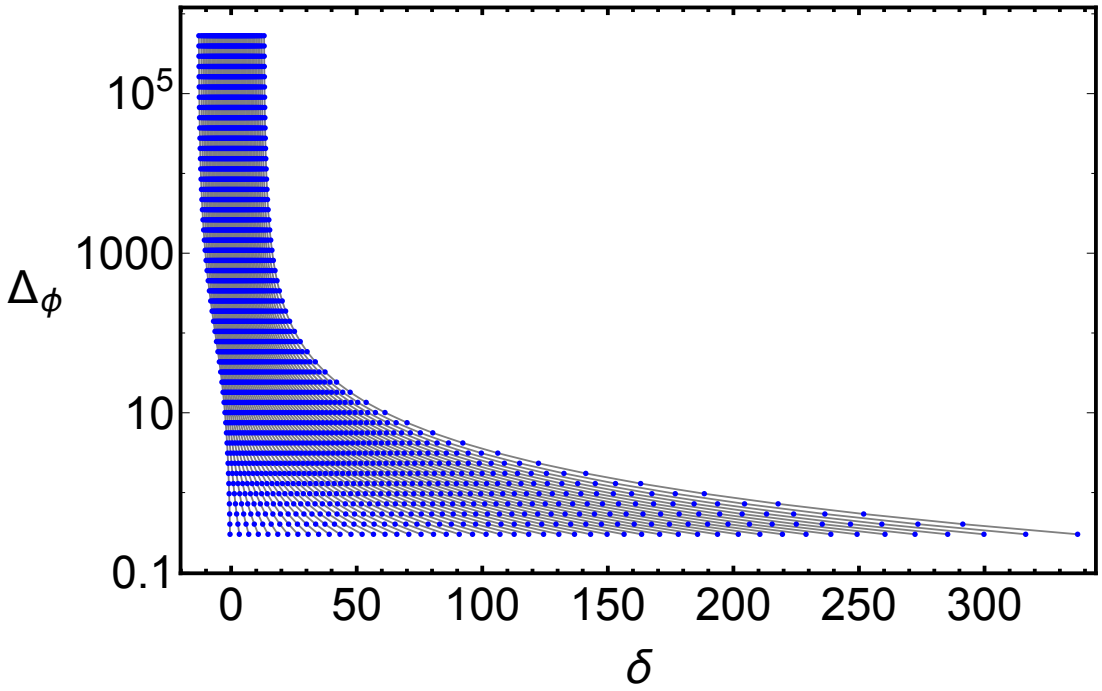

Figure: Flow of the spectrum of operator dimensions as Δ_ϕ is increased. Dimensions of operators are shown in terms of $\delta \equiv (\Delta - 2\sqrt{2}\Delta_\phi)/\sqrt{\Delta_\phi}$. Each horizontal slice is a spectrum at a given Δ_ϕ. For large values of Δ_ϕ the dimensions of operators stabilize in a region with finite width in units of $\sqrt{\Delta_\phi}$ centered at $\delta = 0$.

OPE max

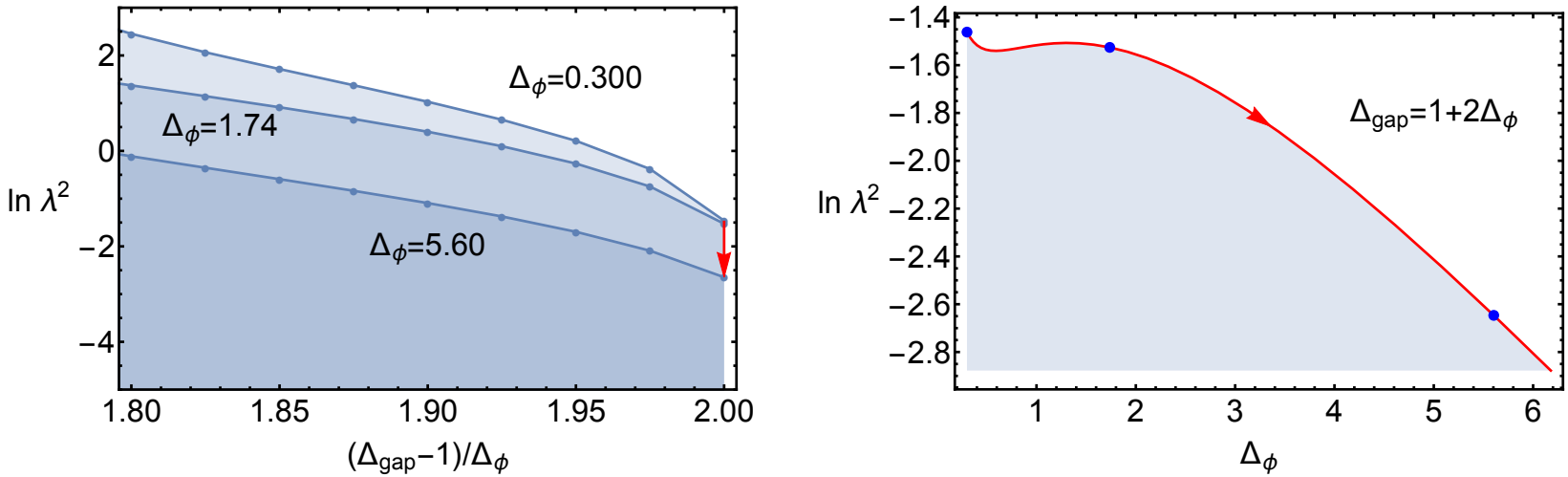

Figure: OPE maximization with $N = 100$ components. On the left, flows from gap maximization to OPE maximization. Given the OPE $\phi \times \phi = \phi + \phi^2 + \ldots$, with $\Delta_{\phi^2} \equiv \Delta_{\text{gap}}$, we are placing an upper bound on $\lambda \equiv \lambda_{\phi\phi\phi}$. On the left, each curve corresponds to a different value for Δ_ϕ, and we vary the gap on the x-axis. On the right, we fix the gap instead to $(\Delta_{\text{gap}} - 1)/\Delta_\phi = 2$ and flow in Δ_ϕ. Hence the red curve on the left plot should match the one on the right. In particular, the blue dots correspond exactly to the intersection of the three curves on the left with the vertical line at $\Delta_{\text{gap}} = 1 + 2\Delta_\phi$.

Non-unitary bootstrap

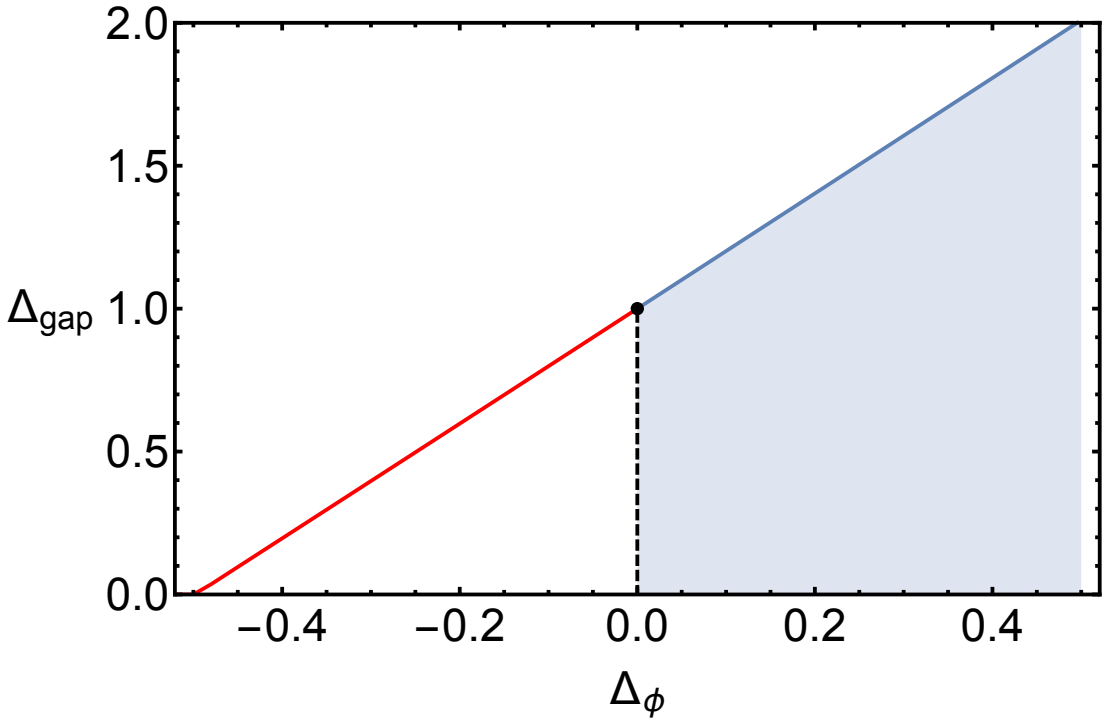

Figure: Flowing into a non-unitary region with $N = 100$ components. Below $\Delta_\phi = 0$ the extremal solution develops a negative OPE coefficient. However, there is still an associated positive linear functional. The functional does set a bound on possible unitary solutions in this region, but this bound may not be optimal.

Non-unitary bootstrap

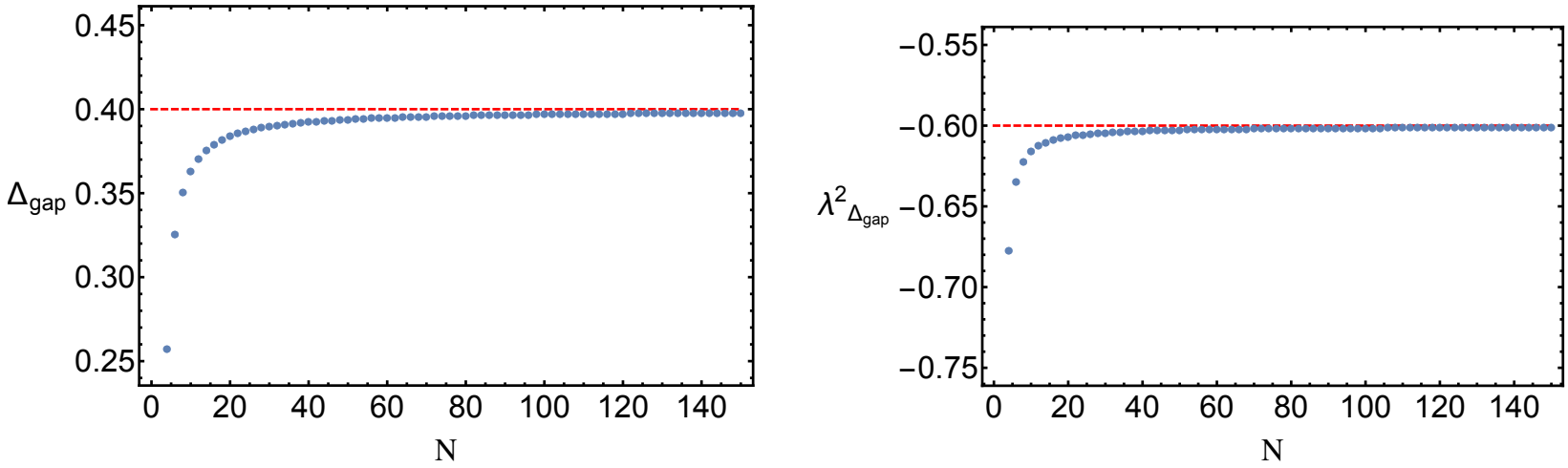

Figure: Upgrading at a non-unitary point, with $\Delta_\phi = -0.3$. On the left, evolution of Δ_{gap} as we increase the number of crosing constraints. The values seem to converge to the correct value $1 + 2\Delta_\phi = 0.4$. Unlike the usual unitary bootstrap, the curve here does not have a meaning of a bound. Accordingly the value Δ_{gap} does not need to decrease as we add more constraints, and in fact here it does the opposite. On the right, the leading, negative, OPE coefficient squared, compared with the exact value $\lambda^2_{j=0} = 2\Delta_\phi = -0.6$.

Non-unitary bootstrap

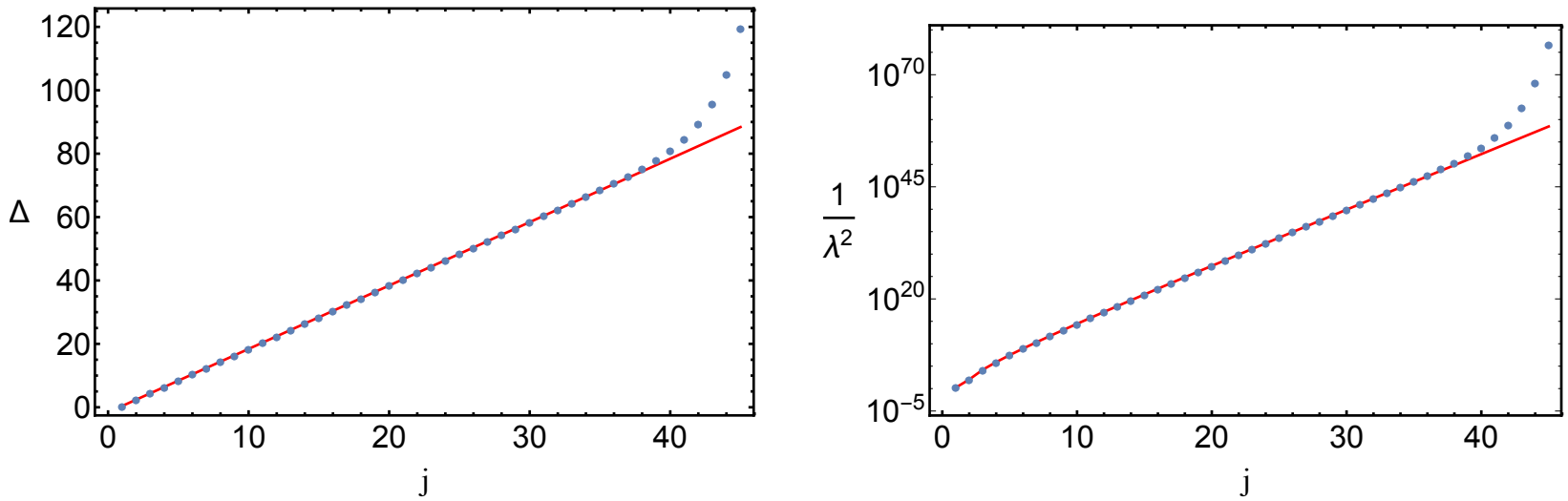

Figure: Upgrading at a non-unitary point: Comparison between the extrapolated spectrum (blue dots) and the exact generalized free fermion (red line). Operators are labeled by an integer j, with $\Delta_j = 1 + 2\Delta_\phi + 2j$. The first 20 operators are correct to better than a part in 10^6. Note that on the right $\lambda^2 < 0$ for $j = 1$ (we are showing it's absolute value).

Singularities

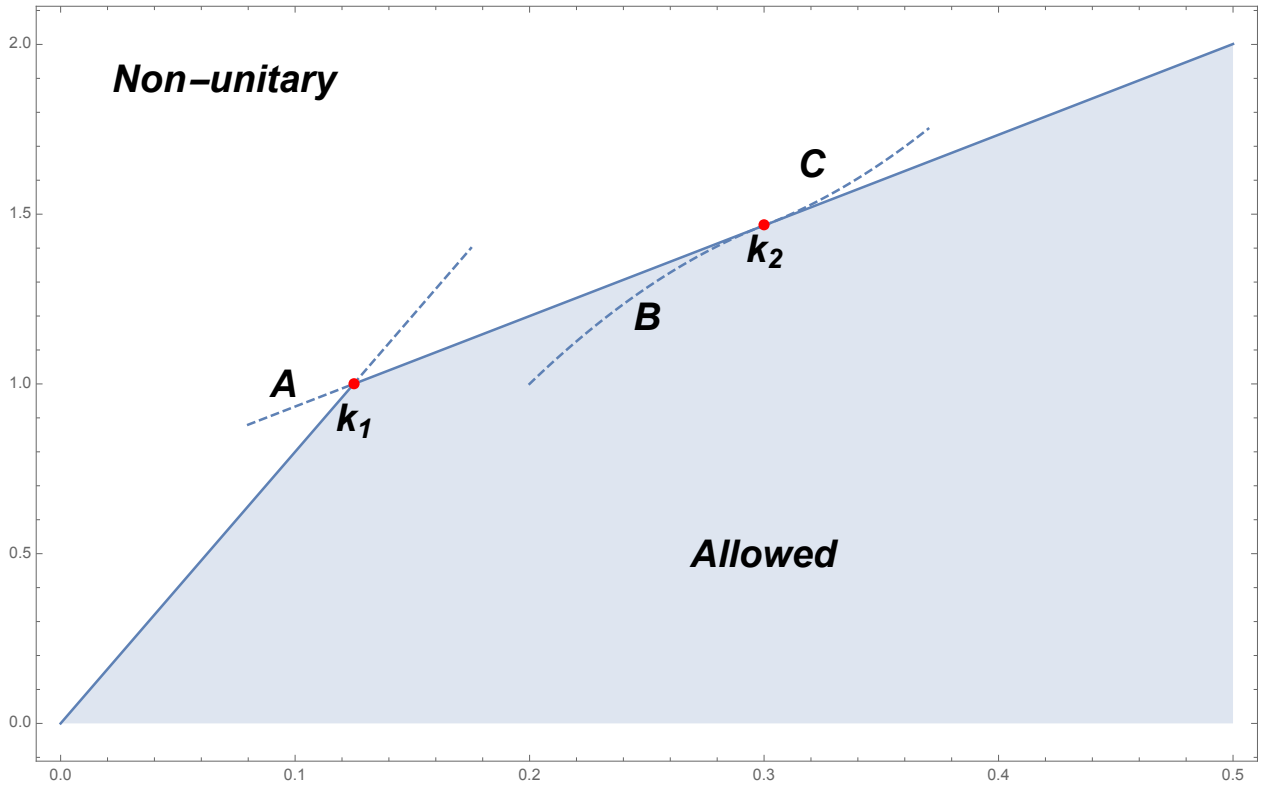

Figure: Singularities and flows (schematic). At an ordinary kink, such as k_1 it is possible to flow into a non-unitary region, say along A, where some OPE coefficient becomes negative. However, not all decouplings of operators signal a visible kink. At when we approach k_2 from the left, an operator decouples. By allowing its OPE to become negative we can flow along C. Conversely, coming from the right, the functional develops a new zero at k_2. If we do not input this new vector into the solution, the latter won't be extremal anymore, and the flow will take us along B.

2d Ising spectrum

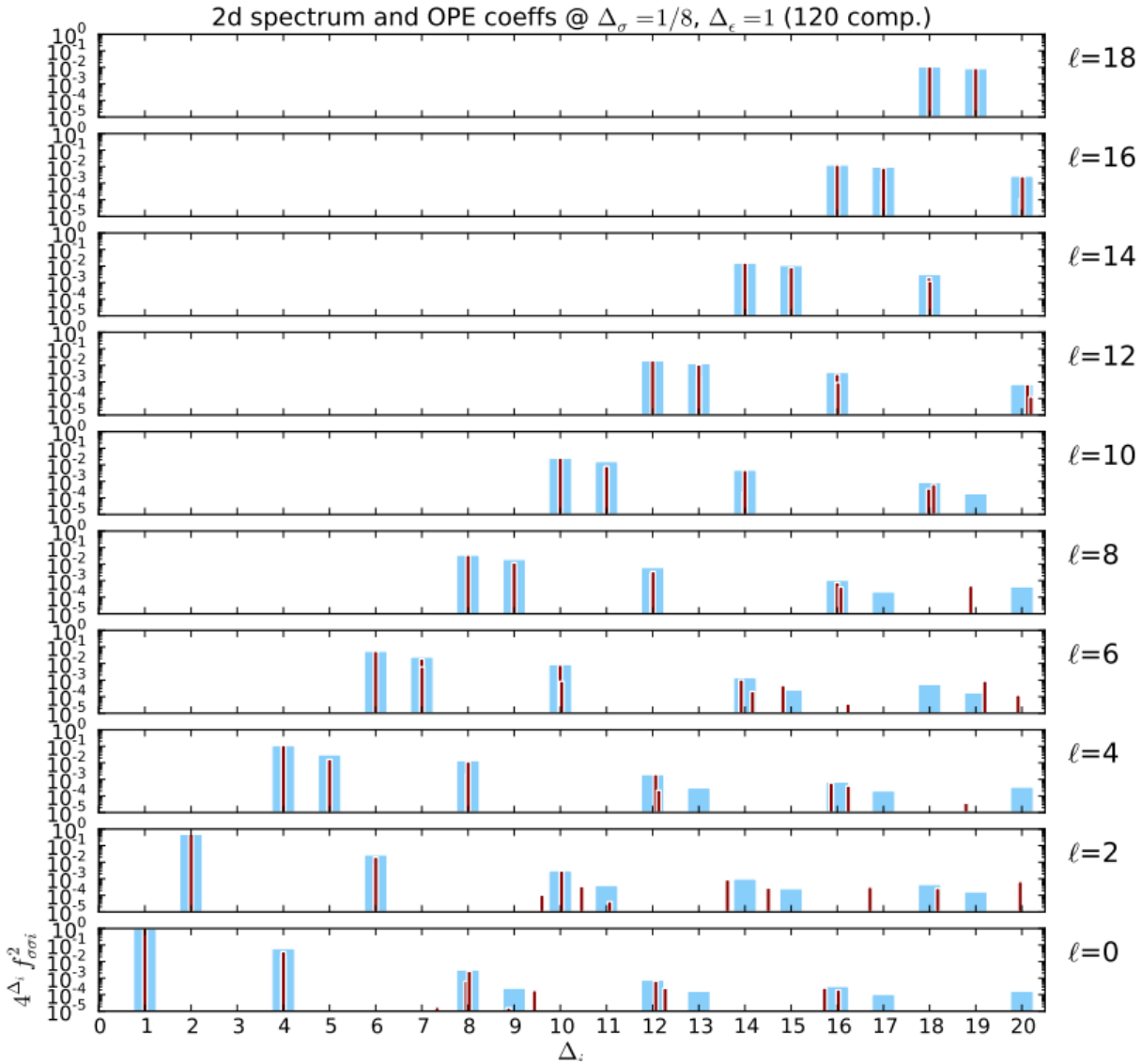

3d Ising: bound on central charge

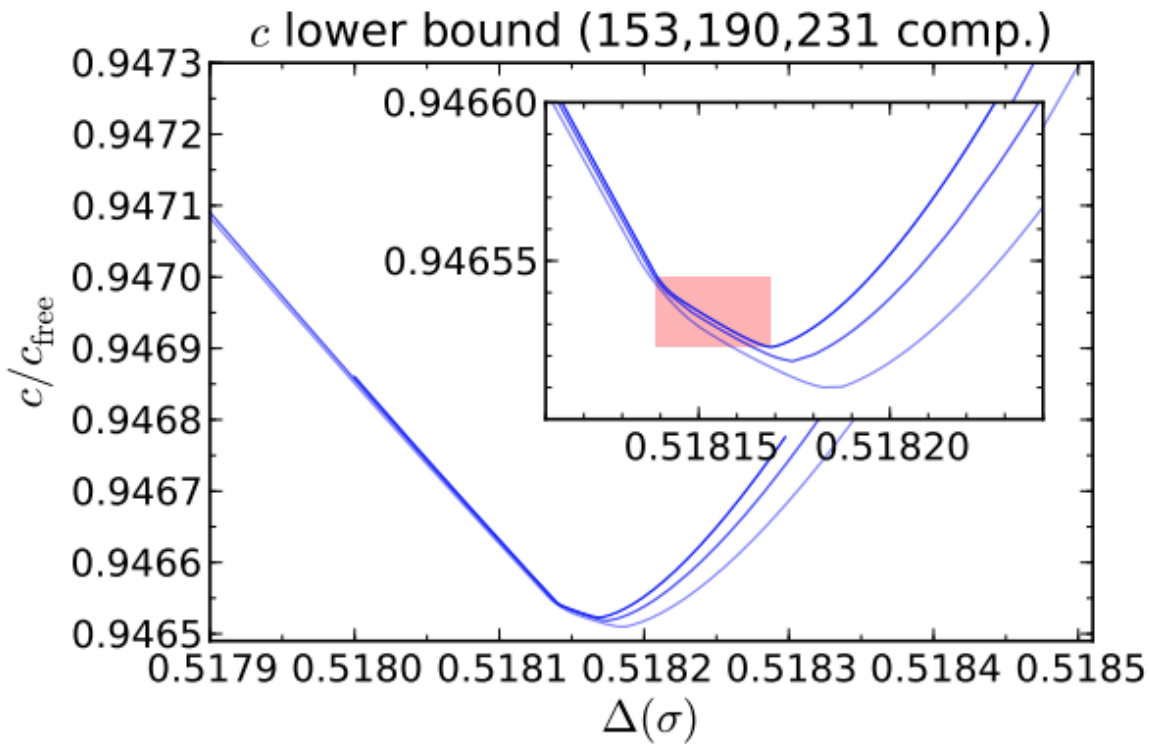

3d Ising: spectrum

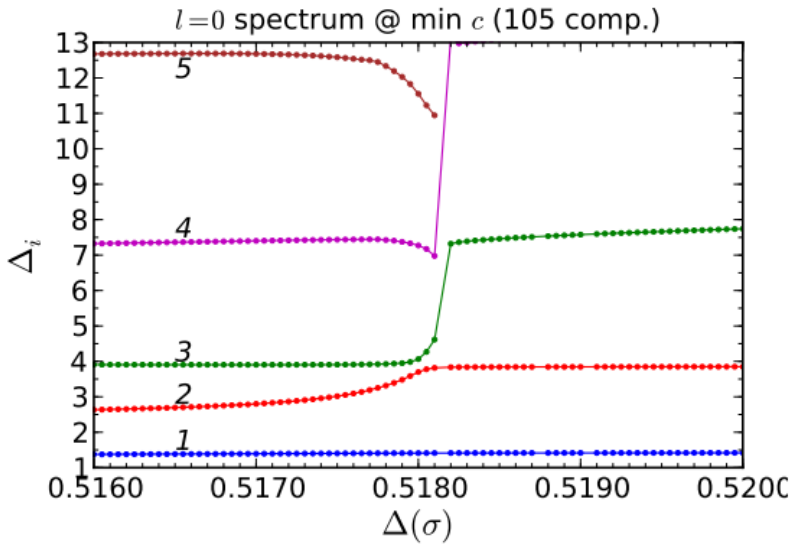

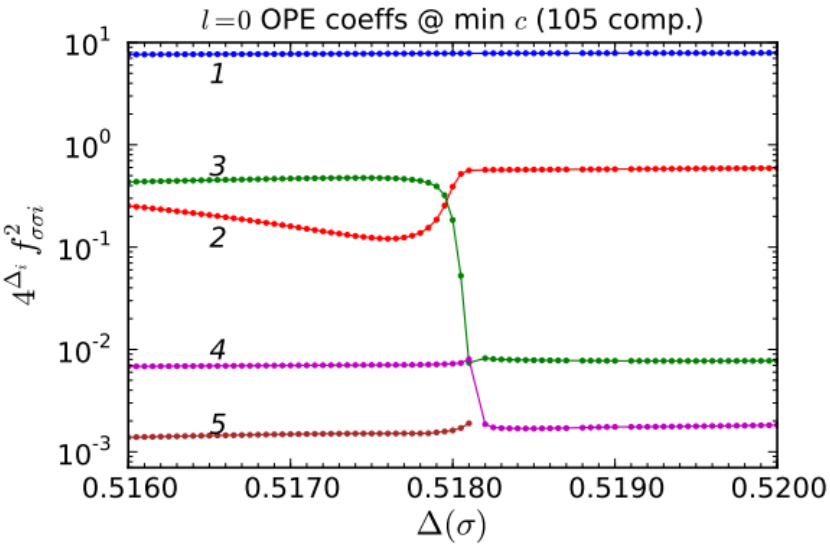

3d Ising: spectrum

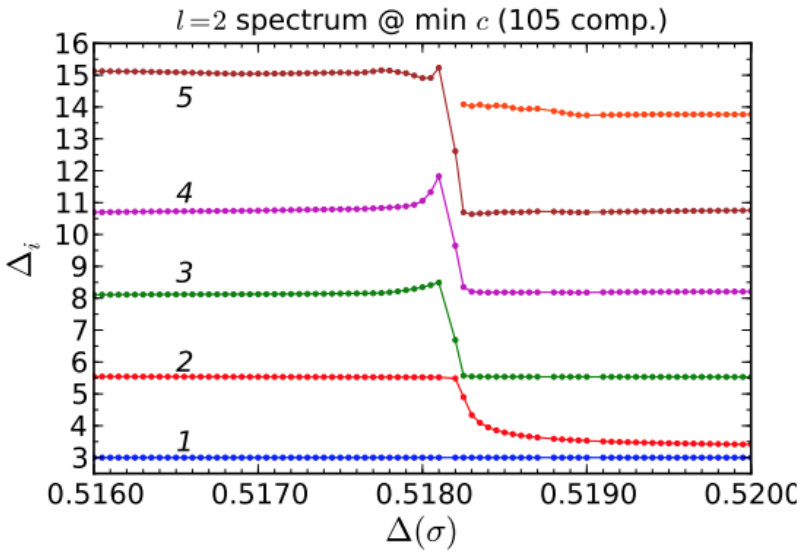

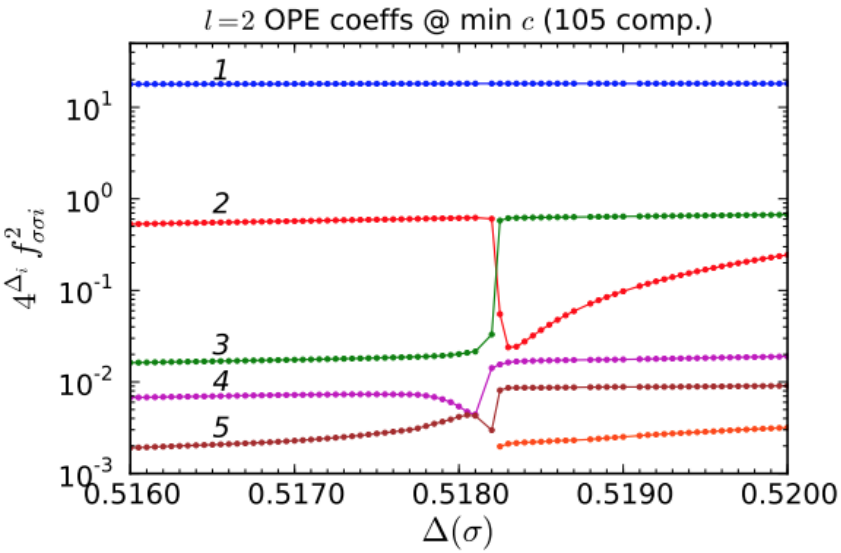

2d Ising: spectrum

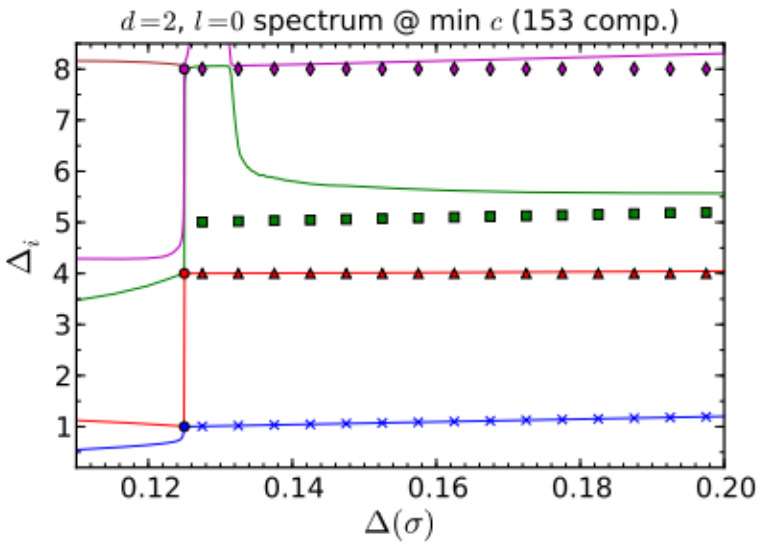

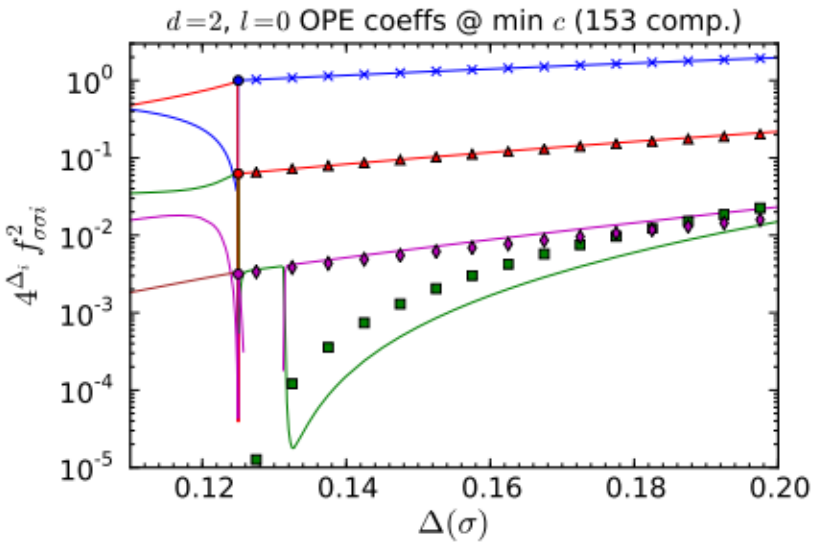

2d Ising: spectrum